

**ANALYSIS OF THE DEDICATED SPECTRAL PHOTOMETRIC OBSERVATIONS FROM MESSENGER'S THIRD MERCURY FLYBY.** Deborah L. Domingue<sup>1</sup>, Scott L. Murchie<sup>2</sup>, Nancy L. Chabot<sup>2</sup>, Brett W. Denevi<sup>3</sup>, Noam R. Izenberg<sup>2</sup>, Gregory M. Holsclaw<sup>4</sup>, <sup>1</sup>Planetary Science Institute, 1700 E. Fort Lowell, Suite 106 Tucson, AZ 85719, E-mail: Domingue@psi.edu, <sup>2</sup>Johns Hopkins University Applied Physics Laboratory, Laurel, MD 20723, <sup>3</sup>School of Earth and Space Exploration, Arizona State University, Box 871404, Tempe, AZ 85287, <sup>4</sup>Laboratory for Atmospheric and Space Physics, University of Colorado, Boulder, CO 80303.

In conjunction with the third flyby of Mercury by the Mercury Surface, Space ENvironment, GEOchemistry, and Ranging (MESSENGER) spacecraft on September 29, 2009, a series of images was taken with the Mercury Dual Imaging System (MDIS) 11-color wide-angle camera (WAC) to systematically measure the disk-integrated brightness of Mercury at solar phase angles between  $\sim 53^\circ$  and  $145^\circ$  at  $1^\circ$ - $2^\circ$  increments. Prior to the third flyby, disk-integrated measurements by MDIS had been acquired at only a handful of solar phase angles. Coupled with measurements taken during the prior two flybys, disk-integrated phase curves can now be constructed in 11 colors ranging from  $\sim 34^\circ$  to  $145^\circ$  phase.

These dedicated photometric observations were obtained in an effort to accurately describe and model the phase function of Mercury's surface in all 11 of MDIS's narrow-band color filters. Analysis of these observations will help provide a more robust photometric model of the color imaging dataset. This is needed for orbital color mapping, in which images obtained at phase angles of  $33^\circ$ - $80^\circ$  will be corrected to a single, common geometry in order to produce a seamless map of color variations among Mercury's surface units. In addition, modeling these phase curves provides a measure of the regolith scattering properties such as roughness, particle scattering function (which relates to particle structure), and single-scattering albedo. Figure 1 is an example of the measured disk-integrated phase curve at 560 nm, compared to Earth-based observations at a similar wavelength [1].

The images used in this photometric analysis were radiometrically calibrated with the current pipeline calibration as described in the Planetary Data System archive. In most of the images, Mercury is only several tens of pixels or less in diameter. Scatter of the signal off the disk by the camera's optics requires integration over a region of the WAC charged-coupled device (CCD) tens to hundreds of times the area of Mercury's disk. Thus, accurate correction for the CCD's background ("dark current") is critical. The pipeline calibration corrects for dark current using a model that incorporates dependence on exposure time, detector temperature, and on-chip binning. An alternate calibra-

tion method corrects for dark current using the values measured from a 4-column strip on the edge of the CCD that is covered with a metallic mask. Reflectance values derived from images using both styles of calibration are nearly identical, so the pipeline calibration method was selected.

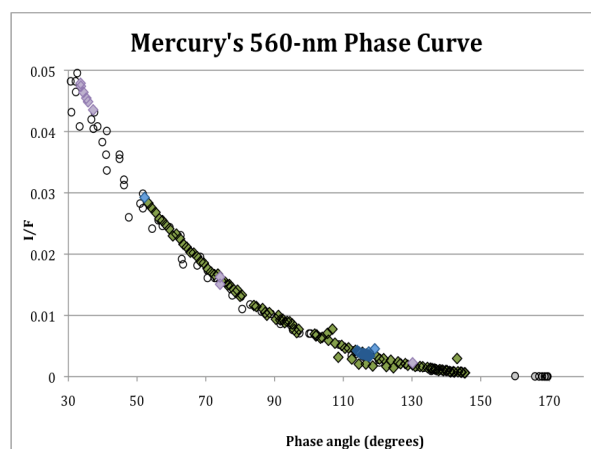


Figure 1. Mercury's disk-integrated reflectance ( $I/F$ , where  $I$  is the amount of light reflected and  $F$  is the incident solar flux times  $\pi$ ) is plotted as a function of solar phase angle. Circles denote Earth-based observations [1] and diamonds represent measurements obtained from the MDIS images. Green diamonds are from the third flyby, purple from the second flyby, and blue from the first flyby.

To assess calibration accuracy, reported values of  $I/F$  of background space were measured and compared with residuals in the dark strip. The background measurements are a residual brightness value from light scattered from Mercury's surface by the camera optics and low level calibration artifacts. These residuals are equivalent to  $I/F$  values of  $10^{-6}$  to  $10^{-8}$  and only significantly affect integrated measurements of reflected light from Mercury when the number of pixels on Mercury's disk is small ( $<50$ ) and the dimensions of the box enclosing scattered light is large (such as in a  $200 \times 200$  pixel box or larger). In order to include as much of the scattered light as possible, but minimize the contribution from calibration artifacts, the disk-integrated brightness was derived by summing the brightness values in a box centered on Mercury that was ten times Mercury's radius in pixels. The number of pixels in

that box was then multiplied by a residual background brightness value (derived from measuring the average background in four 100 x 100 pixel boxes at the corners of each image), and this value was subtracted from the summed brightness value. The result was then divided by the number of pixels containing Mercury's disk to provide the disk-integrated brightness. Estimates of the measurement uncertainties are less than 5%.

The modeling parameters, in addition to providing insight into the regolith particle properties, enable the photometric correction of spectral measurements derived from the images. Besides supporting future orbital mapping, this correction facilitates comparison of multispectral imaging measurements with the higher-spectral-resolution visible-infrared spectral measure-

ments from MESSENGER's Mercury Atmospheric and Surface Composition Spectrometer (MASCS) Visible and Infrared Spectrometer (VIRS). By identifying VIRS measurement locations on MDIS images obtained during flyby 2, MDIS broadband spectra and corresponding VIRS spectra were extracted. Figure 2 is a comparison of two spectra taken at similar illumination and viewing geometries. The photometric correction derived from the disk-integrated data enable comparisons of VIRS spectra with broadband spectra derived from MDIS that are taken at different illumination and viewing geometries.

**References:** [1] Mallama, A., et al. (2002) *Icarus*, 155, 253-264.

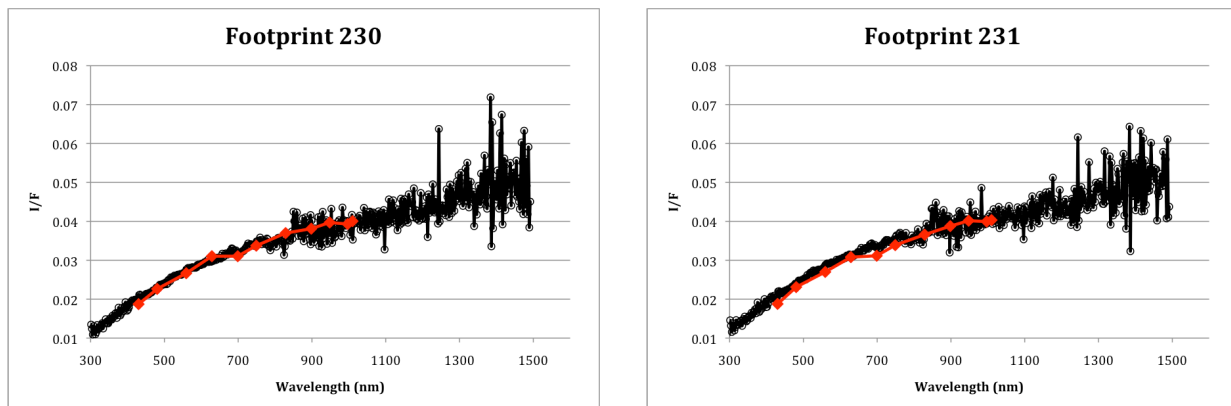


Figure 2. Comparison of two VIRS spectra (black circles) with corresponding MDIS (red diamonds) imaging spectra of the same area.